Inhomogeneous electronic properties of monolayer graphene on Ru(0001)

M. Gyamfi, T. Eelbo, M. Waśniowska,[*] and R. Wiesendanger

Institute of Applied Physics, University of Hamburg, Jungiusstrasse 11, D-20355 Hamburg, Germany
(Received 19 February 2011; published 26 April 2011)

Scanning tunneling microscopy and scanning tunneling spectroscopy (STS) at low temperatures were applied to prove lateral inhomogeneities in the electronic properties of a single layer of graphene on the Ru(0001) surface. We found two different types of STS curves depending on the location within the moiré pattern of graphene, providing direct proof for coupled and uncoupled parts of monolayer graphene on Ru(0001). Moreover, we observed differences in dI/dU curves between hills, valleys, and rims of hills, and we discuss them in relation to the electronic bulk states of Ru(0001). A detailed analysis revealed that graphene's dominating STS peak at -0.4 eV originates from a d-like Ru bulk state.

Studies of graphene revealed a range of new phenomena caused by the uniqueness of such a low-dimensional material with low energy excitations resembling massless Dirac fermions.[1] Understanding the properties of the interface between graphene and a metal has recently gained considerable attention due to the fact that graphene could be a promising candidate for future nanoscale electronics. Since nanoscale electronics require contacts between a graphene sheet and metal electrodes, it is essential to have a full understanding of the physics of metal-graphene interfaces. Moreover, gate voltages or metal electrodes[2] can change freestanding graphene with the Dirac point at the Fermi energy to either p-doped or n-doped systems. Additionally, interest in the graphene-metal interface stems from the catalytic synthesis of carbon nanotubes for which metal particles are used during the growth process. For these reasons, the interfaces between graphene and metallic surfaces, e.g., Rh,[3] Ni,[4] or Ir,[5] represent very flexible model systems for studying the influence of the atomic and electronic structures on electrical contacts with graphene-related systems.

For monolayer graphene (MLg) on Ru(0001), as reported previously by various groups, a moiré pattern with a 3.0 nm distance between hills is observed in scanning tunneling microscopy (STM),[6–8] low electron energy diffraction (LEED),[9] and surface x-ray diffraction (SXRD) studies.[10] Moreover, the carbon atoms in MLg/Ru(0001) are electronically inequivalent as revealed by x-ray core-level photoelectron spectroscopy, which shows two peaks. These two peaks are related to the hills and valleys of the moiré pattern, i.e., two areas of differently bonded C atoms.[11] Detailed insight into the growth and the electronic properties of this system has been obtained by STM experiments at room temperature[6] and 55 K.[7] Low-bias scanning tunneling spectroscopy (STS) experiments performed at room temperature reveal the existence of a spatial charge redistribution in the graphene layer, showing an electronic difference between hills and valleys. STM images of areas with monolayer graphene, shown in Ref. 7, are often dominated by a strong contrast related to the electronic properties, i.e., depending on the bias voltage, the STM topography shows a rim surrounding the hills. This rim is a result of laterally inhomogeneous electronic properties, which can be interpreted as evidence of a strong interaction between graphene and Ru in apparent agreement with the ultraviolet photoemission spectroscopy (UPS) results.[12,13] The UPS study together with

theoretical calculations confirms strong bonding between the graphene layer and Ru, i.e., strong hybridization between C $2p_z$ and Ru $4d_{z^2}$ orbitals. Due to this hybridization the linear dispersion is not any more preserved for MLg. However, in UPS experiments the electronic properties of several carbon units are averaged on length scales much larger than the atomic scale. Therefore, high-resolution measurements of the electronic properties are highly desirable. The purpose of this paper is to show direct evidence for variations of the electronic properties regarding the exact position of the carbon rings of a graphene sheet with respect to the ruthenium atoms within the subunit cell. The electronic states at -0.40, $+0.2$, and $+0.55$ eV observed by means of STS are identified as bulk states of Ru(0001). The STS measurements are compared with theoretical calculations performed in Refs. 14 and 15.

All experiments have been carried out in an ultrahigh vacuum system with separate chambers for sample preparation and low-temperature STM measurements. The Ru(0001) single crystal was cleaned by repeated cycles of Ar$^+$-ion sputtering at 300 K and subsequent annealing. Graphene was prepared by thermal decomposition of C_2H_4 on the Ru(0001) surface.[16] The STM/STS measurements were performed at 30 K. We used several tungsten tips for investigating the electronic structure of the combined graphene/Ru system. All dI/dU spectra were measured by adding a modulation voltage $U_{mod} = 20$ mV$_{rms}$ with a frequency of 3.7 kHz to the applied sample bias U and recording the dI/dU signal by a lock-in technique to obtain information about the local density of states (LDOS).

An overview of MLg on the Ru(0001) surface is shown in Fig. 1(a). The topography shows that in addition to the MLg, small areas of the clean ruthenium surface are visible. Atomic resolution of the Ru(0001) substrate and the MLg on the terrace shows undistorted hexagonal order for both surfaces [cf. Figs. 1(b)–1(e)]. However, very close to the edge of MLg islands the Ru surface is distorted and exhibits defects [cf. the inset in Fig. 1(a)], which supports the conclusion that the Ru layer underneath graphene is corrugated.[9,17]

The superstructure moiré pattern, which is a fingerprint of graphene on Ru(0001), is clearly observed on the MLg islands in Fig. 1(a) with the atomically resolved subunit cell of the moiré structure presented in Figs. 1(b) and 1(c). However, Fig. 2 displays bias voltage-dependent atomic resolution images of graphene's superstructure. The STM data sets
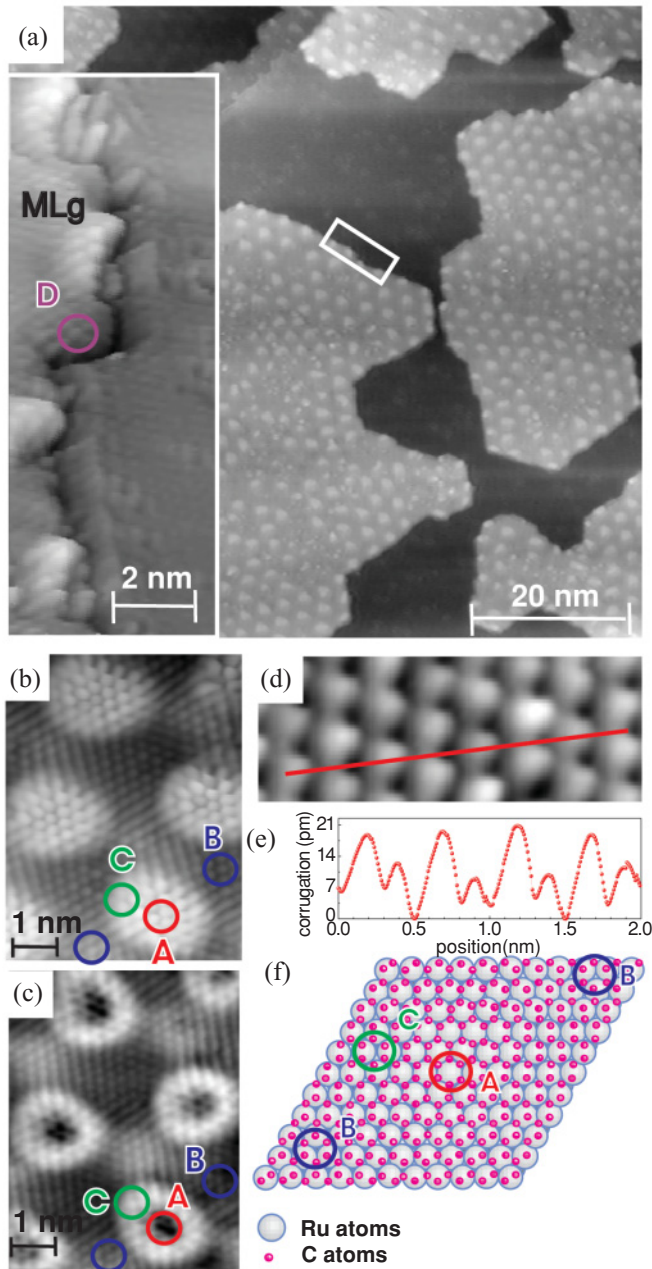
FIG. 1. (Color online) Morphology of monolayer epitaxial graphene (MLg) on Ru(0001). (a) STM image of a large area of monolayer epitaxial graphene. The inset shows a magnified view of the border region of the MLg and Ru terrace indicated in (a). Tunneling parameters are $U = 0.5$ V and $I = 1$ nA. (b) and (c) High-resolution STM images of the same part of the moiré structure of the graphene layer ($U = +0.2$ V, $I = 0.2$ nA and $U = +0.6$ V, $I = 0.5$ nA, respectively). (d) The atomically resolved topography showing hollow sites of Ru(0001) and the corresponding line profile (e). The scan size is 2.5×0.5 nm. Tunneling parameters are $I = 0.5$ nA and $U = 200$ mV. (f) Corresponding model of MLg on Ru(0001).
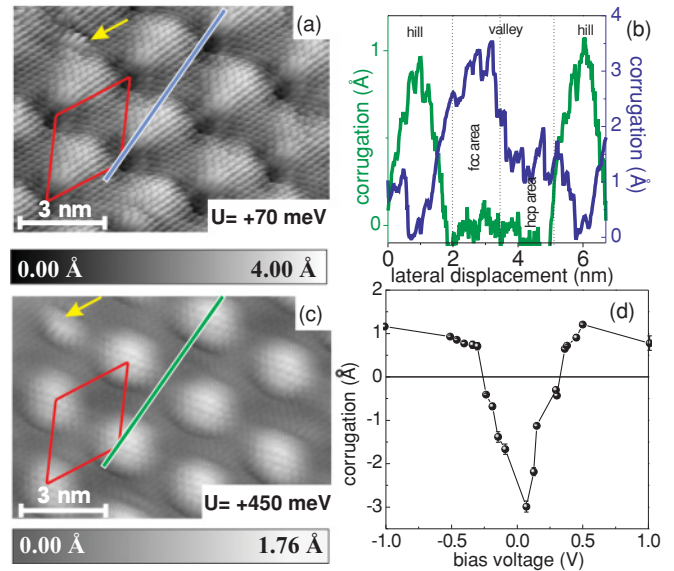

FIG. 2. (Color online) Atomically resolved STM images of graphene on Ru(0001) obtained with a W tip indicating that the contrast inversion depends on the tunneling parameters. The tunneling current was 0.5 nA. In (a) and (c) the yellow arrows denote a defect in the moiré pattern as a position marker for the superstructure. The subunit cell is shown as a red rhombus. (b) Line profiles along the lines indicated in (a) and (c). (d) Evolution of the apparent corrugation of the moiré pattern with the sample bias. The corrugation was measured between the hill and the fcc area of the valley.

were taken at the same sample position, marked by a defect (yellow arrow). The moiré pattern is imaged in two different ways: the hills are imaged as bright protrusions [Fig. 2(c)] or dark depressions [Fig. 2(a)], depending on the bias voltage. Additionally, the corrugation of the moiré pattern varies with

the bias voltage, as shown in Figs. 2(b) and 2(d). The height difference is up to 3 Å. Interestingly, we found a decrease of the corrugation of the upper areas in the moiré pattern contrary to the lower areas [cf. Fig. 2(d)] in the bias range from -0.3 to $+0.3$ eV. This is surprising because previous STM experiments[18] clearly showed that the corrugation of hills is reversed only at high voltages around $+2.8$ eV. Moreover, the contrast in our STM data within the valleys of the moiré pattern is not changed with the bias voltage, revealing that only hills are influenced by this electronic effect in STM measurements.

To gain a full understanding of the atomically resolved images presented in Figs. 2 and 1(c), structural as well as electronic information of the MLg subunit cell are needed. According to previous experimental results[6,7] and theoretical predictions,[14,19] regions with high (hills) and low (valleys) areas are observed, due to surface relaxation. The valleys contain carbon rings centered on fcc or hcp hollow sites with respect to the substrate, contrary to hills where rings are centered on the top positions of the Ru atoms. In between these areas the carbon rings are centered on bridge positions forming structural domain walls[20] [cf. Fig. 1(f)].

To understand the electronic properties of the moiré pattern observed in our STM data we performed STS on the lower and upper sites of the superstructure and the clean Ru surface. STS measurements of Ru(0001) were used as a reference. Figures 3(a) and 3(b) show the simultaneously acquired dI/dU spectra as a function of bias on the clean Ru(0001) and on graphene, respectively. dI/dU spectra for clean Ru(0001) exhibit a prominent peak at $U = -0.4$ V and another two peaks corresponding to unoccupied states at $U = +0.2$ and $+0.55$ V.
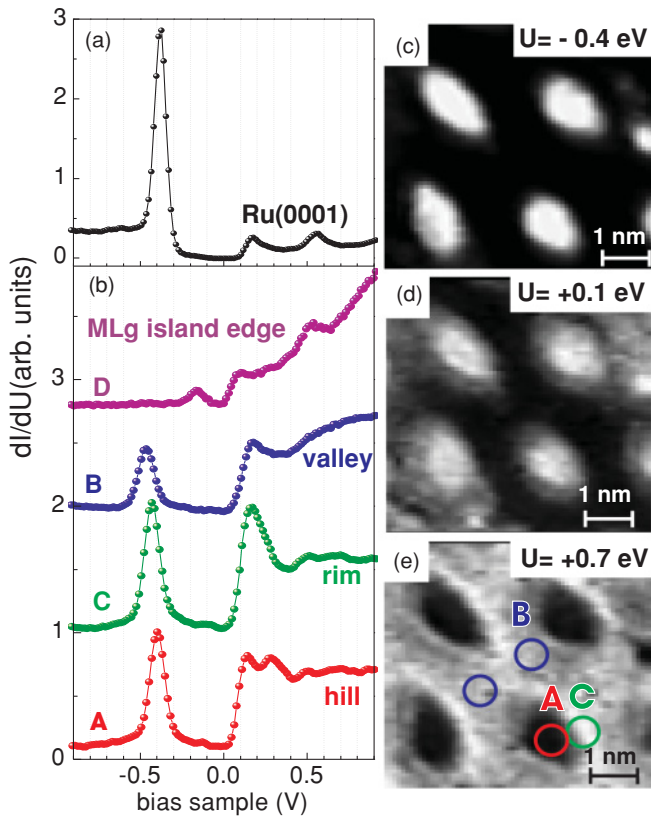
FIG. 3. (Color online) (a) Tunneling spectra of the Ru(0001) surface with visible bulk states. (b) The tunneling curves recorded on edges of the MLg island, hills, valleys, and rim positions. Spectrum D is taken on the area indicated in the inset of Fig. 1(a). The STS curves are shifted by offsets of 0.9 arb. units with respect to one another. Tunneling parameters for STS are $I = 0.5$ nA and $U = 1$ V. (c)–(e) Spatial map of the tunneling conductance of the subunit cell.

We note that the ruthenium spectrum was measured far away from graphene islands.

In order to support the interpretation of the measured spectrum on the Ru surface, we compare dI/dU curves on the ruthenium surface with inverse photoemission spectroscopy (IPS) and UPS data from Ref. 21 and Refs. 22 and 13, respectively. The UPS and IPS experiments together with theoretical band-structure calculations of the Ru(0001) surface[15] show evidence of bulk d-like states close to the Fermi energy and a surface state at -2.5 eV. In Fig. 3(a), we identify the topmost d-like state for the clean Ru surface at -0.40 eV, in agreement with UPS experiments,[13,22] while for unoccupied states, at a considerably lower bias, we find two peaks ($+0.2$ and $+0.55$ eV) which can be related to the d states of Ru,[21] as well. By making use of the comparison between UPS and IPS with STS, the above-mentioned features are unambiguously identified as a manifestation of the Ru(0001) bulk states. Usually, dI/dU spectra reflect features in the LDOS of the surface at the position of the tip that are related to surface states or resonances, and very rarely with the local density of bulk states.[23] But indeed, contributions from bulk states were already observed for metals in the past [Ni(111) (Ref. 24), Nb(011) (Ref. 25)]. Furthermore, we compare our experimental data with the calculated LDOS of the Ru surface

from Ref. 14, which shows several peaks at occupied states, while for unoccupied states peaks appear at $+0.5$ and $+1.2$ eV. Apart from a shift by about 0.2 eV for the state observed in our experimental data at -0.40 eV, there is good qualitative agreement between the theoretical and the measured spectrum of Ru for electronic states at $+0.5$ and -0.7 eV.

In order to get access to the local variations of the electronic structure inside the moiré pattern we performed spatially resolved STS, as shown in Fig. 3(b). The very high lateral resolution of the spectroscopic field enables us to assign the spectra taken on the MLg to a certain stacking sequence. The dI/dU curves in Fig. 3(b) are averaged over areas indicated by A, B, C, and D in Figs. 1(b) and 1(c). Curve A represents hills, while B belongs to valleys. We do not observe differences in the spectra of carbon rings located on fcc or hcp hollow sites as well as on bridge positions in between them. Therefore, only the averaged curve (B) is shown in Fig. 3(b). The lack of any electronic difference becomes even more obvious when inspecting the dI/dU maps in Figs. 3(c)–3(e). The dI/dU spectrum of the edge of MLg (curve D) shows a shoulder at $+0.55$ eV and two symmetric peaks around the Fermi energy. The comparison of spectra of the MLg edge with MLg and Ru curves, which are simultaneously taken, let us exclude tip contributions. While the general curvature of the dI/dU spectra is quite similar on all parts of the moiré pattern, the spectra differ by a shift, $\Delta E = 30$ meV, of the peak position at -0.4 eV and its intensity. This small energy difference is related to the hybridization of carbon and Ru atoms upon adsorption of graphene on the Ru surface. Despite a different shape of the dI/dU curve measured on MLg in comparison to experimental results from Ref. 6, an asymmetry in the energy range close to the Fermi energy is visible, i.e., a higher LDOS of empty states in the valleys and higher LDOS of filled states in the hills. We note that in contrast to the theoretical calculations,[14] none of our STS measurements shows a peak at the Fermi energy. If we compare the spectra of hills and valleys of the moiré pattern with the rims separating them we can observe that the rims have identical spectra to the valleys, while they electronically differ from the hills [cf. Fig. 3(b)]. However, the dI/dU curve of the hills is different for unoccupied states. We find a minimum at $+0.2$ eV, where a sharp peak is observed in the spectra of other parts of the moiré pattern. dI/dU spectra exhibit the minimum at $+0.2$ eV for several (5–9) carbon rings of the hills, depending on the size and shape of the ripple [cf. Fig. 1(d)]. We attribute this minimum to the Dirac point, which was predicted in Ref. 12. In their calculations, the simplest configuration of the hills' band structure is the one of freestanding unsupported MLg with the Dirac point at approximately $+0.3$ eV. Additionally, a small feature can be observed in the spectra obtained on rims and hills at -0.12 eV. We relate this peak to a phonon-mediated inelastic channel[26–28] because this feature is neither observed on the clean Ru surface nor on lower areas of MLg [cf. Fig. 3(a)]. The observation of phonon excitations indicates that the graphene in the top position of the hills is decoupled from the Ru substrate.

In order to visualize the interplay between structural and electronic properties of the moiré pattern we display dI/dU maps at selected energies in Figs. 3(c)–3(e); the corresponding voltages are indicated in Fig. 3. The first dI/dU map, which is

presented in Fig. 3(c), is taken at -0.4 eV and shows a contrast between hills and valleys only. Additionally, in Fig. 3(e), a contrast between the rim and the central part of the hills is visible. In this dI/dU map we observe that bright rims appear around the central part of the hills, which are observed in STM topography [see Fig. 1(c) and Ref. 7]. We attribute these rims to carbon rings located on the bridge positions between the hills (top positions) and valleys (fcc and hcp hollow sites) according to the structural model in Ref. 20 and Fig. 1(f). Due to the strain relief of hills of the moiré pattern, this bridge position shows different bonding to the Ru substrate than the bridge position between fcc and hcp hollow sites in the valleys of the superstructure. Since STM does not directly image the topography of the surface, but rather the electronic density of states, a difference in bonding of carbon atoms to ruthenium results in different apparent heights of hills, valleys, and rims. For this reason the electronic contribution is enhanced in dI/dU maps and STM topography.

In summary, we demonstrated that the electronic structure of the MLg on Ru(0001) changes significantly on the length scale of only a few carbon rings. The main difference of the electronic structure is, on the one hand, at occupied states, i.e., a shift of the dominating peak at -0.4 eV on hills which shifts to lower energies for valleys. On the other hand, at unoccupied states, only hills have a minimum at $+0.2$ eV. A detailed analysis revealed that the dominant peak originates from a d-like Ru bulk state. The spectroscopic shift between differently stacked areas results from different hybridization of the Ru bulk states with graphene states. We assume that MLg hills are in equilibrium distance from the Ru surface and that the Dirac point is located at $+0.2$ eV, revealing that hills are p-type doped by the metal substrate.

*mwasniwo@physnet.uni-hamburg.de

[1] A. H. C. Neto, F. Guinea, N. M. R. Peres, K. S. Novosolev, and A. K. Geim, Rev. Mod. Phys. **81**, 109 (2009).

[2] Y. Zhang, V. W. Brar, F. Wang, C. Girit, Y. Yayon, M. Panlasigui, A. Zettl, and M. F. Crommie, Nat. Phys. **4**, 627 (2008).

[3] B. Wang, M. Caffio, C. Bromley, H. Früchtl, and R. Schaub, ACS Nano **4**, 5773 (2010).

[4] A. Nagashima, N. Tejima, and C. Oshima, Phys. Rev. B. **50**, 17487 (1994).

[5] A. T. N'Diaye, J. Coraux, T. N. Plasa, C. Busse, and T. Michely, New J. Phys. **10**, 043033 (2008).

[6] A. L. Vazquez de Parga, F. Calleja, B. Borca, M. C. G. Passeggi, J. J. Hinarejos, F. Guinea, and R. Miranda, Phys. Rev. Lett. **100**, 056807 (2008).

[7] S. Marchini, S. Günther, and J. Wintterlin, Phys. Rev. B **76**, 075429 (2007).

[8] E. Sutter, D. Acharya, J. Sadowski, and P. Sutter, Appl. Phys. Lett. **94**, 133101 (2009).

[9] W. Mortiz, B. Wang, M. L. Bocquet, T. Brugger, T. Greber, J. Wintterlin, and S. Günther, Phys. Rev. Lett. **104**, 136102 (2010).

[10] D. Martoccia *et al.*, Phys. Rev. Lett. **101**, 126102 (2008).

[11] A. B. Preobrajenski, M. L. Ng, A. S. Vinogradov, and N. Martensson, Phys. Rev. B **78**, 073401 (2008).

[12] T. Brugger, S. Günther, B. Wang, H. Dil, M. L. Bocquet, J. Osterwalder, J. Wintterlin, and T. Greber, Phys. Rev. B **79**, 045407 (2009).

[13] P. Sutter, M. S. Hybertsen, J. T. Sadowski, and E. Sutter, Nano Lett. **9**, 2654 (2009).

[14] B. Wang, M. L. Bocquet, S. Marchini, S. Günther, and J. Wintterlin, Phys. Chem. Chem. Phys. **10**, 3530 (2008).

[15] N. A. W. Holzwarth and J. R. Chelikowsky, Solid. State Commun. **53**, 171 (1985).

[16] P. W. Sutter, J. I. Flege, and E. A. Sutter, Nat. Mater. **7**, 406 (2008).

[17] D. Martoccia, M. Björck, C. M. Schlepütz, T. Brugger, S. A. Pauli, B. D. Patterson, T. Greber, and P. R. Willmott, New J. Phys. **12**, 043028 (2010).

[18] B. Borca, S. Barja, M. Garnica, J. J. Hinarejos, A. L. V. de Parga, R. Miranda, and F. Guinea, Semicond. Sci. Technol. **25**, 034001 (2010).

[19] X. Peng and R. Ahuja, Phys. Rev. B **82**, 045425 (2010).

[20] D. E. Jiang, M. H. Du, and S. Dai, J. Chem. Phys. **130**, 074705 (2009).

[21] W.-K. Siu and R. A. Bartynski, Phys. Rev. B **75**, 235427 (2007).

[22] T. Pelzer, G. Ceballos, F. Zbikowski, B. Willerding, K. Wandelt, U. Thomann, C. Reuß, T. Fauster, and J. Braun, J. Phys.: Condens. Matter **12**, 2193 (2000).

[23] J. Tersoff and D. R. Hamann, Phys. Rev. B **31**, 805 (1985).

[24] Y. Nishimura, M. Kakeya, M. Higashiguchi, A. Kimura, M. Taniguchi, H. Narita, Y. Cui, M. Nakatake, K. Shimada, and H. Namatame, Phys. Rev. B **79**, 245402 (2009).

[25] B. Koslowski, C. Dietrich, and P. Ziemann, Surf. Sci. **557**, 255 (2004).

[26] V. W. Brar *et al.*, Phys. Rev. Lett. **104**, 036805 (2010).

[27] M.-C. Wu, Q. Xu, and W. Goodman, J. Phys. Chem. **98**, 5104 (1994).

[28] Y. Liu, L. Zhang, M. K. Brinkley, G. Bian, T. Miller, and T.-C. Chiang, Phys. Rev. Lett. **105**, 136804 (2010).